Supplemental information

Store-operated Ca^{2+} entry regulates Ca^{2+}-activated chloride channels and eccrine sweat gland function

Axel R. Concepcion, Martin Vaeth, Larry E. Wagner II, Miriam Eckstein, Lee Hecht, Jun Yang, David Crottes, Maximilian Seidl, Hyosup P. Shin, Carl Weidinger, Scott Cameron, Stuart E.Turvey, Thomas Issekutz, Isabelle Meyts, Rodrigo S. Lacruz, Mario Cuk, David I. Yule, and Stefan Feske

Authorship note: A.R. Concepcion and M. Vaeth contributed equally to this work.

Correspondence should be addressed to: S. Feske, Department of Pathology, New York University School of Medicine, 550 First Avenue, Smilow 316, New York, NY 10016, USA. Phone: 212.263.9066; Email: feskes01@nyumc.org.

Table of contents:

Supplemental Methods

NCL-SG3 cells and shRNA transduction. NCL-SG3 cells were cultured in complete William's E medium (Sigma) supplemented with 5% fetal bovine serum (Gibco), 1% penicillin-streptomycin and 1% L-glutamine (both from Corning), 1X insulin-transferrin-selenium (ITS) supplement and 20 ng/ml epidermal growth factor (both from Life Technologies), and 10 ng/ml hydrocortisone (Sigma). For knockdown of ORAI1, STIM1, BEST2 and TMEM16A expression, NCL-SG3 cells were stably transduced with lentiviral particles expressing ORAI1, STIM1, BEST2 or TMEM16A-specific shRNAs (Supplemental Table 1). Briefly, HEK293FT packaging cells were co-transfected with lipid-polymer/DNA complexes using GenJet transfecting reagent (SignaGen Laboratories) and miR-E11 SGEP-GFP-PGK-puromycin lentiviral vector (1), psPAX2 packaging (Addgene, 12260) and pMD2.G VSV-G envelope expressing plasmids (Addgene, 12259). Lentiviral particles harvested at day 2 and 3 were used to transduce NCL-SG3 cells after spin-infection with 8 µg/ml polybrene (EMD Millipore). Transduced NCL-SG3 cells were selected for 3 days with 5 µg/ml puromycin and the purity of cells was confirmed by flow cytometry and detection of GFP expression.

Flow cytometry. shRNA-mediated knockdown of ORAI1 protein in NCL-SG3 cell lines was confirmed by flow cytometry. Briefly, NCL-SG3 cell lines were incubated for 15 min at 25 µg/ml with a custom-made mouse anti-human ORAI1 monoclonal antibody (clone 29A2) that recognizes the second extracellular loop of hORAI1. Mouse IgG1 Ab (25 µg/ml) was used as isotype control. After 15 min, cells were stained with a goat anti-mouse IgG-Alexa Fluor 647 secondary antibody (1:500 dilution, Life Technologies) for 15 min and ORAI1 expression was analyzed using a FACS LSR II flow cytometer (BD Biosciences) and FlowJo software (Tree Star).

Western blotting. NCL-SG3 cells stably transduced with shSTIM1 and shTMEM16A were cultured in 6-well plates to confluency and lysed with 500 µl of 1X Laemmli sample buffer (5% β-mercaptoethanol, 0.0005% bromophenol blue, 10% glycerol, 2% SDS, 63 mM Tris-HCl, and 1% protease inhibitor cocktail, pH 6.8, all from Sigma). Samples were sonicated for 15 min and heated at 95 °C for 15 min (STIM1) or left unheated (TMEM16A). Cell debris was removed by centrifugation at 15,000 x *g* for 5 min. Protein extracts were separated by SDS-PAGE using precast NuPAGE 4-12% Bis-Tris gradient gels (Invitrogen) and transferred to

nitrocellulose membranes. After blocking, membranes were incubated overnight with a custom-made rabbit anti-human STIM1 polyclonal antibody (1:1000) that recognizes the C terminus of STIM1 (2), rabbit anti-human TMEM16A polyclonal antibody (1:1000, ab84115, Abcam) or goat anti-Actin polyclonal antibody (1:200, I-19; Santa Cruz Biotechnology) as loading control. After incubation with IRDye 680LT donkey anti-rabbit or IRDye 800CW donkey anti-goat secondary antibodies (1:10,000, Licor) for 2 h, immunoreactive bands were detected with an Odyssey Fc Western Blot Detection System (Licor Bioscience). Band densities were quantified and analyzed using ImageJ 1.50i.

Sweat testing. The footpads of anesthetized mice were first painted with 2% (w/v) iodine/ethanol solution and then with 1 g/ml starch/castor oil solution (Sigma). After drying, 50 µl of 100 µM acetylcholine (Sigma) was injected subcutaneously into the paws of mice. Pictures of the mouse footpads were taken after 5 min using a SteREO Discovery V8 microscope (Zeiss). For sweat tests using the CRAC channel inhibitor BTP2 (EMD Millipore, catalog number 203890), 1 or 100 µM BTP2 or vehicle (ethanol) were applied epicutaneously to the footpad skin of mice for 4h or 2h before the beginning of the sweat test. The numbers of sweat dots on mouse paws were counted by multiple investigators in a blinded manner and averaged.

Histology, immunohistochemistry, immunofluorescence and image analysis. Tissue specimens were fixed in 4% PFA and embedded in paraffin. Heat-induced antigen retrieval of samples was performed in 10 mM citric acid buffer (pH 6.0) for 20 min using a high-pressure cooker (Deni). Blocking for 1 h with Antibody Diluent (Dako) was followed by overnight incubation at 4°C with the following primary antibodies: affinity-purified rabbit polyclonal anti-ORAI1 (3) (1:50 dilution), rabbit polyclonal anti-STIM1 (1:200, Sigma), rabbit anti-TMEM16A/ANO1 (1:50, a gift of Dr. Lily Jan, University of California, San Francisco, CA (4)), rabbit polyclonal anti-BEST2 (1:100, H-188, sc98568; Santa Cruz Biotechnology), and rabbit polyclonal anti-human TMEM16A (1:50, ab84115; Abcam). Detection was carried out using donkey anti-rabbit IgG (H+L) conjugated either with AlexaFluor555 or AlexaFluor488 (both 1:800) for immunofluorescence (IF) microscopy. For immunohistochemistry, samples were incubated with anti-rabbit-biotin (1:500) for 30 min followed by Neutravidin-HRP (1:500, both Pierce) for 45 min. DAB Substrate (Sigma) was incubated until saturation of the staining and tissue was subsequently counterstained with hematoxylin as described (5). Slides were mounted using Prolong Gold Antifade Mounting Medium containing DAPI (Molecular Probes) for detection using IF or

Vectamount embedding medium (Vector Laboratories) for light microscopy, respectively. Slides were analyzed on a Nikon Eclipse E600 fluorescence microscope with NIS Elements BR 3.2 (Nikon) software or with an automated laser-scanning confocal microscope (Leica TCS SP5 II equipment). Images of skin biopsies stained with H&E were scanned using a SCN400 slide scanner (Leica) and analyzed using Slidepath Digital Image Hub (Leica). To measure sweat gland lumen area, skin biopsies images were analyzed using ImageJ 1.50i. by setting the pixels in length scale (μm) and manually drawing the perimeter of the sweat gland lumens to calculate the lumen area (μm^2). Between 2-5 coiled nests of eccrine sweat gland structures were analyzed per human or mouse skin sample. The number of skin samples is indicated in the figure legends.

Measurement of intracellular Ca^{2+} levels in isolated sweat glands and cell lines. Sweat glands isolated from mice were seeded onto UV-sterilized coverslips pre-coated with Cell-Tak (Corning) and loaded with 1 μM Fura-2-AM (Life Technologies) and 0.5 μM CellTracker Orange CMRA (Invitrogen) for 30 min, and $[Ca^{2+}]_i$ was analyzed using time-lapse imaging on an IX81 epifluorescence microscope (Olympus). Each sweat gland was marked by a region of interest. The ratio of Fura-2 emission following excitation at 340 nm (F340) and 380 nm (F380) were calculated for each time point and analyzed using SlideBook imaging software v4.2 (Olympus). For measurements of SOCE, baseline $[Ca^{2+}]_i$ was acquired in nominally Ca^{2+}-free Ringer solution (155 mM NaCl, 4.5 mM KCl, 3 mM $MgCl_2$, 10 mM D-glucose, and 5 mM Na-HEPES, pH 7.4) followed at the indicated times by stimulation with 1 μM acetylcholine to deplete ER stores. To induce Ca^{2+} influx, cells were perfused with Ca^{2+}-containing Ringer solution (155 mM NaCl, 4.5 mM KCl, 2 mM $CaCl_2$, 1 mM $MgCl_2$, 10 mM D-glucose, and 5 mM Na-HEPES, pH 7.4). For $[Ca^{2+}]_i$ measurements in NCL-SG3 cells, F340/F380 ratios were measured in Fura-2–loaded cells with a FlexStation 3 multi-mode microplate reader (Molecular Devices) as described (6). Briefly, NCL-SG3 cell lines loaded with 1 μM Fura-2-AM were plated on poly-L-lysine–coated translucent 96-well plates (BD Falcon) for 15 min, and incubated in 0 mM Ca^{2+} Ringer solution for 10 min before measurements of $[Ca^{2+}]_i$. Store depletion was induced by stimulating the cells with 1 μM ionomycin (Invitrogen) in 0 mM Ca^{2+} Ringer solution and Ca^{2+} influx was induced after adding an equal volume of 2 mM $CaCl_2$ Ringer solution to the cells (to obtain a final extracellular $[Ca^{2+}]$ of 1 mM). Alternatively, Ca^{2+} imaging was performed in Fura-2–loaded NCL-SG3 cell lines on glass coverslips using an inverted epifluorescence Nikon microscope with a 40x oil immersion objective (NA=1.3). Loaded cells were perfused with HEPES imaging buffer

containing 137 mM NaCl, 4.7 mM KCl, 1.26 mM $CaCl_2$, 1 mM Na_2HPO_4, 0.56 mM $MgCl_2$, 10 mM HEPES, and 5.5 mM glucose, pH 7.4, and stimulated with 10 μM trypsin (Thermo Fisher Scientifics). Images were captured every second with an exposure of 10 ms and 4x4 binning using a digital camera driven by TILL Photonics software. All measurements of intracellular $[Ca^{2+}]_i$. levels were performed at room temperature (22–25 °C). $[Ca^{2+}]_i$ was calculated from F340/F380 ratios and calibration curves generated using the Calcium Calibration Buffer Kit#1 (Molecular Probes, Life technologies) as described (7). Ca^{2+} store depletion and influx were quantitated by measuring peaks values of $[Ca^{2+}]_i$ and the area-under-the-curve (AUC) after subtracting the $[Ca^{2+}]_i$ baseline.

Measurement of intracellular Cl^- levels in isolated sweat glands and cell lines. Isolated murine sweat glands were adhered to Cell-Tak pre-coated coverslips and loaded with 5 mM MQAE (Biotium) for 30 min, and $[Cl^-]_i$ was analyzed using time-lapse microscopy. MQAE emission at 460 nm was measured after excitation at 360 nm using an IX81 epifluorescence microscope (Olympus). For measurements of $[Cl^-]_i$, baseline $[Cl^-]_i$ was acquired in Cl^--containing solution (96 mM NaCl, 5.3 mM KCl, 0.8 mM MgSO4, 1 mM NaH_2PO_4, 1.8 mM calcium acetate, 50 mM mannitol, 22 mM $NaHCO_3$, 5.6 mM D-glucose, and 5 mM HEPES, pH 7.4) followed at the indicated times by stimulation with 1 μM acetylcholine. To maximize Cl^- efflux, sweat glands were perfused with isoosmotic Cl^--free buffer solution containing isethionate (101.3 mM Na-isethionate, 0.8 mM MgSO4, 1 mM NaH_2PO_4, 1.8 mM calcium acetate, 50 mM mannitol, 16.7 mM $NaHCO_3$, 5.3 mM $KHCO_3$, 5.6 mM D-glucose, and 5 mM HEPES, pH 7.4). The $[Cl^-]_i$ in sweat glands was estimated from calibration curves performed on MQAE-loaded glands by using the double ionophore technique (5 μM nigericin and 10 μM tributyltin in high-K^+ media) and the Stern-Volmer equation $[Cl^-]_i = [(F_0/F)-1]/K_{Cl}$ as described (8). K_{Cl} is the Stern-Volmer quenching constant for Cl^- (K_{Cl} = 3.7 M^{-1}) and F_0/F is the ratio of emitted fluorescence in the absence and presence of Cl^- in the extracellular media. To measure $[Cl^-]_i$ in NCL-SG3 cells adherent on poly-L-lysine coated coverslips, the same protocol as above was used with the exception that cells were stimulated with 1 μM ionomycin. All measurements of intracellular Cl^- levels were performed at room temperature (22–25 °C). For quantitation of $[Cl^-]_i$, Cl^- efflux rates (slopes) were defined as changes in $[Cl^-]_i$ after ACh stimulation or perfusion with Cl^--free buffer and calculated by linear regression analysis of values recorded at the indicated time-points. Changes in $[Cl^-]_i$ defined as integrated area were calculated as the area below or above the curve

(relative to the baseline of $[Cl^-]_i$ defined as the mean of $[Cl^-]_i$ between 0-90s) after ACh stimulation or removal of extracellular Cl^-. The net Cl^- efflux for each condition was calculated as the difference between the baseline in $[Cl^-]_i$ at the beginning of the experiment (defined as described before) and ACh stimulation (defined as the mean of $[Cl^-]_i$ between 150-350s), or the end (defined as the mean of $[Cl^-]_i$ between 500-700s) of the experiment, respectively.

Supplemental References

1. Fellmann C, Hoffmann T, Sridhar V, Hopfgartner B, Muhar M, Roth M, Lai DY, Barbosa IA, Kwon JS, Guan Y, et al. An optimized microRNA backbone for effective single-copy RNAi. *Cell reports.* 2013;5(6):1704-13.

2. Maus M, Jairaman A, Stathopulos PB, Muik M, Fahrner M, Weidinger C, Benson M, Fuchs S, Ehl S, Romanin C, et al. Missense mutation in immunodeficient patients shows the multifunctional roles of coiled-coil domain 3 (CC3) in STIM1 activation. *Proceedings of the National Academy of Sciences of the United States of America.* 2015;112(19):6206-11.

3. McCarl CA, Picard C, Khalil S, Kawasaki T, Rother J, Papolos A, Kutok J, Hivroz C, Ledeist F, Plogmann K, et al. ORAI1 deficiency and lack of store-operated Ca^{2+} entry cause immunodeficiency, myopathy, and ectodermal dysplasia. *The Journal of allergy and clinical immunology.* 2009;124(6):1311-8 e7.

4. Huang F, Rock JR, Harfe BD, Cheng T, Huang X, Jan YN, and Jan LY. Studies on expression and function of the TMEM16A calcium-activated chloride channel. *Proceedings of the National Academy of Sciences of the United States of America.* 2009;106(50):21413-8.

5. Vaeth ME, M. Shaw, P. Kozhaya, L. Yang, J. Berberich-Siebelt, F. Clancy, R. Unutmaz, D. Feske, S. Store-operated Ca^{2+} entry in follicular T cells controls humoral immune responses and autoimmunity *Immunity.* 2016;44(6):1350-64.

6. Weidinger C, Shaw PJ, and Feske S. STIM1 and STIM2-mediated Ca^{2+} influx regulates antitumour immunity by $CD8^+$ T cells. *EMBO molecular medicine.* 2013;5(9):1311-21.

7. Nurbaeva MK, Eckstein M, Concepcion AR, Smith CE, Srikanth S, Paine ML, Gwack Y, Hubbard MJ, Feske S, and Lacruz RS. Dental enamel cells express functional SOCE channels. *Scientific reports.* 2015;(5)15803.

8. Bevensee MO, Apkon M, and Boron WF. Intracellular pH regulation in cultured astrocytes from rat hippocampus. II. Electrogenic Na/HCO3 cotransport. *The Journal of general physiology.* 1997;110(4):467-83.

Supplemental Table 1. Sense strand shRNA sequences

Gene target	Oligonucleotides
Ren.713 (Renilla luciferase, control)	5'-CAGGAATTATAATGCTTATCTA-3'
BEST2.182 (human)	5'-ATTCGAGAAGCTTGTGATTTAT-3'
ORAI1.1270 (human)	5'-CGTCCTCTAAGAGAATAAGCAT-3'
STIM1.4008 (human)	5'-CCCCATTTTCATGTTACTTTGT-3'
TMEM16A.3628 (human)	5'-CCCTCCTAATTCCTTAAGATAG-3'

Supplemental Table 2. Specific primers designed for qRT-PCR.

Human transcript	Oligonucleotides
AQP5	5'-AGAATCAGCTCCACCACCAT-3' (sense) 5'-CTGGCATCCTCTACGGTGT-3' (antisense)
BEST2	5'-CGCTGGAACTGCATGTCTT-3' (sense) 5'-ACAGCGGCTACTGTCTTCCA-3' (antisense)
CFTR	5'-CCACTCAGTGTGATTCCACCT-3' (sense) 5'-ACAGAAGCGTCATCAAAGCA-3' (antisense)
FOXA1	5'-GCCTGAGTTCATGTTGCTGA-3' (sense) 5'-CTGTGAAGATGGAAGGGCAT-3' (antisense)
GAPDH	5'-TCCAAAATCAAGTGGGGCGA-3' (sense) 5'-AAATGAGCCCCAGCCTTCTC-3' (antisense)
ORAI1	5'-GATGAGCCTCAACGAGCACT-3' (sense) 5'-ATTGCCACCATGGCGAAGC-3' (antisense)
SLC12A1	5'-CAGCTGAACTTGGGGTGACT-3' (sense) 5'-ACTATCGTAACACCGGCAGC-3' (antisense)
SLC12A2	5'-ATTTGCAAAGCCATCCTCAA-3' (sense) 5'-ATCACTACCGGCACACAGC-3' (antisense)
STIM1	5'-ACACAGGGGCTTGTCAATTC-3' (sense) 5'-GTCACAGTGAGAAGGCGACA-3' (antisense)
TMEM16A	5'-CCTCTTCCTCTTCAAAGCCC-3' (sense) 5'-TCTCTGTCTTCATGGCCCTC-3' (antisense)
TMEM16B	5'-GGTAACCTGGGAAACGATCC-3' (sense) 5'-CAACCAGTCTGCTGTCCAGA-3' (antisense)
Mouse transcript	Oligonucleotides
Aqp5	5'-TAGAAGATGGCTCGGAGCAG-3' (sense) 5'-CTGGGACCTGTGAGTGGTG-3' (antisense)
Best2	5'-CTATGCACATGAGTGCGTCC-3' (sense) 5'-TCATCCCCGTCTCTTTCGTA-3' (antisense)
Cftr	5'-CCTCAAAATTGGTGTGGTCC-3' (sense) 5'-CACAGACCTCATTGCCTCAC-3' (antisense)
Foxa1	5'-TGGAGTTCATAGAGCCCAGG-3' (sense) 5'-CATGAGAGCAACGACTGGAA-3' (antisense)
Hprt	5'-AGCCTAAGATGAGCGCAAGT-3' (sense) 5'-TTACTAGGCAGATGGCCACA-3' (antisense)
Orai1	5'-AGACTGCCTGATCGGATGGC-3' (sense) 5'-TTGTCCCCGAGCCATTTCCT-3' (antisense)
Orai2	5'-GCAGCTACCTGGAACTCGTC-3' (sense) 5'-GTTGTGGATGTTGCTCACCG-3' (antisense)
Orai3	5'-CAGTCAGCACTCTCTGCGG-3' (sense) 5'-TGGCCACCATGGCGAAG-3' (antisense)
Slc12a1	5'-GCCAATCTCTCCTGTTCCAG-3' (sense) 5'-TGGCGTGGTCATAGTCAGAA-3' (antisense)
Slc12a2	5'-TACTCTCGGCAGTGTATGCG-3' (sense) 5'-CTCCACGATGAGCTGGAAA-3' (antisense)
Stim1	5'-ATTCGGCAAAACTCTGCTTC-3' (sense) 5'-GGCCAGAGTCTCAGCCATAG-3' (antisense)
Stim2	5'-TCGAAGTGGACGAGAGTGATG-3' (sense) 5'-TTTCCACTGTTTCCACAAATCC-3' (antisense)
Tmem16a	5'-ATGTTCACGATGTGGACGC-3' (sense) 5'- GCAGGAACCCCCAACTCA-3' (antisense)
Tmem16b	5'-GCTGACTTGCCACTCTCCTT-3' (sense) 5'-CTGACTGGGATCGAAGAGGA-3' (antisense)

Supplemental Figure 1

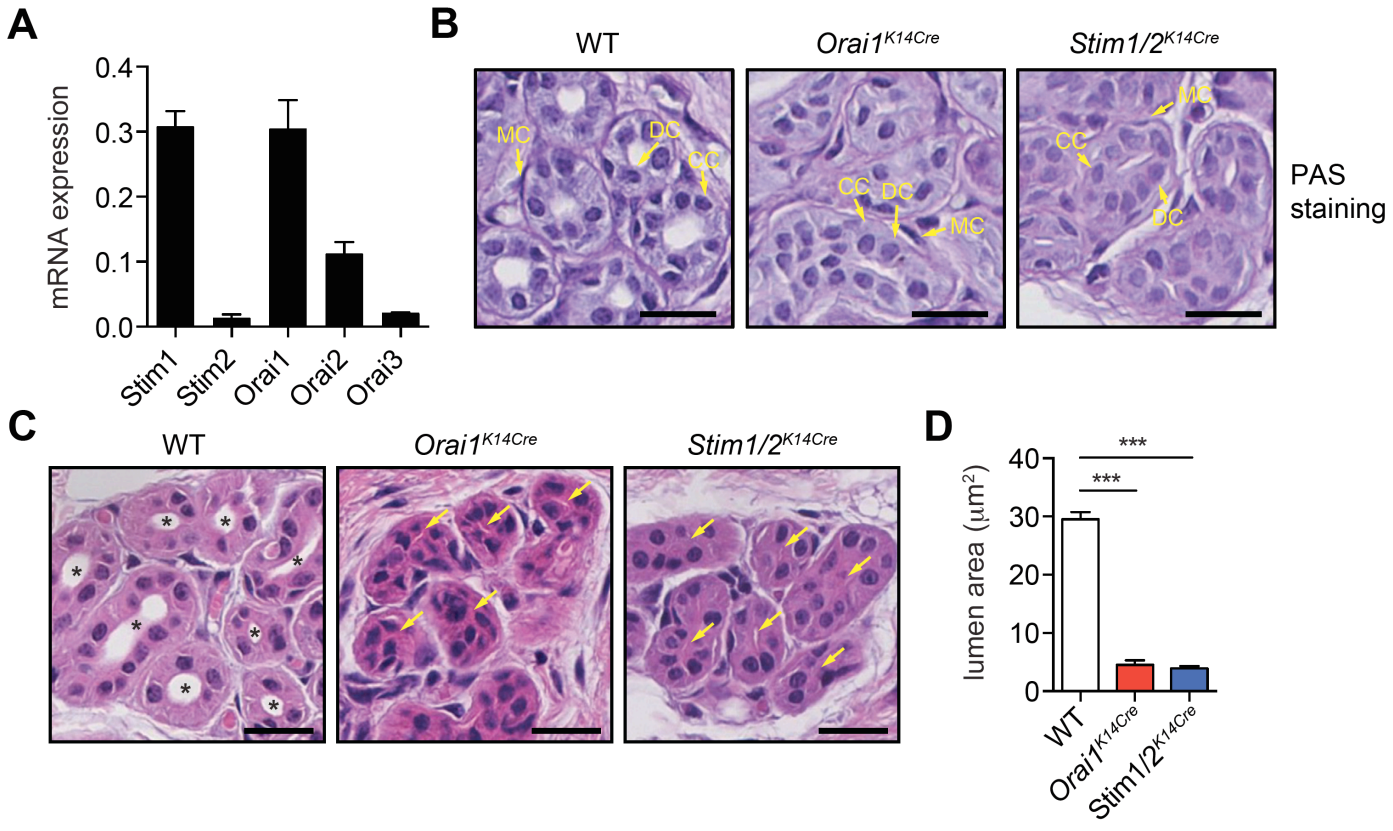

Supplemental Figure 1. ORAI1 and STIM1/STIM2 are not required for sweat gland development in mice. (**A**) mRNA expression of CRAC channel genes in sweat glands isolated from paws of WT mice analyzed by qRT-PCR. Hypoxanthine guanine phosphoribosyl transferase (*Hprt*) was used to normalize expression. Data shown are mean ± SEM of 14 WT mice. (**B**) Periodic acid-Schiff (PAS) staining of mouse skin tissue from the hind paws of WT, *Orai1*^{K14Cre}, and *Stim1/2*^{K14Cre}. Yellow arrows indicate the different cell types in the secretory portion of the sweat glands (CC, clear cells; DC, dark cells; and MC, myoepithelial cells). Images are representative of 2 mice per genotype. Scale bars, 20 µm. (**C**) H&E staining of hind paw skin biopsies of WT, *Orai1*^{K14Cre} and *Stim1/2*^{K14Cre} mice. Scale bars, 20 µm. Arrows indicate residual sweat gland lumens. (**D**) Quantification of the sweat gland lumen area of the mouse skin biopsies similar to those shown in **C**. Bars represent the mean of 8 WT, 4 *Orai1*^{K14Cre}, and 4 *Stim1/2*^{K14Cre} mice. Between 4-5 coiled nests of eccrine sweat glands were analyzed per skin biopsy. Statistical analyses were performed by 2-tailed Student's *t* test. ***P<0.001.

Supplemental Figure 2

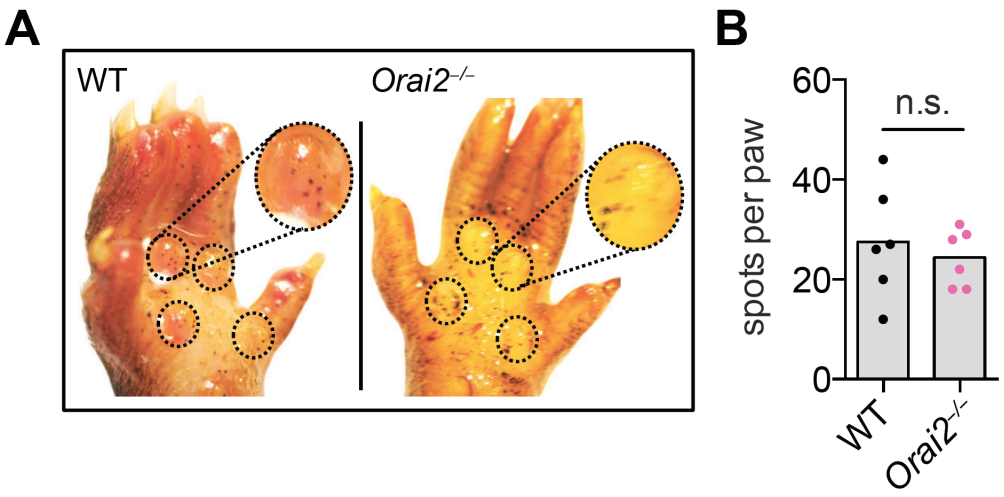

Supplemental Figure 2. ORAI2 is not required for sweat gland function in mice. (**A**) Representative images of ACh-induced sweat response in the hind paw of WT and *Orai2*$^{-/-}$ mice visualized by the starch-iodine sweat test. Images from the mouse paws 5 min after 100 μM ACh injection are shown. (**B**) Number of black dots counted in the digits of the mouse paws after 5 min of ACh injection in WT (n = 3) and *Orai2*$^{-/-}$ (n = 3) mice. Each dot represents the number of responder glands in one of the hind paw of one mouse and both hind paws per mouse are plotted in the graph. No significant (n.s.) differences between genotypes were observed by Student's 2-tailed t test.

Supplemental Figure 3

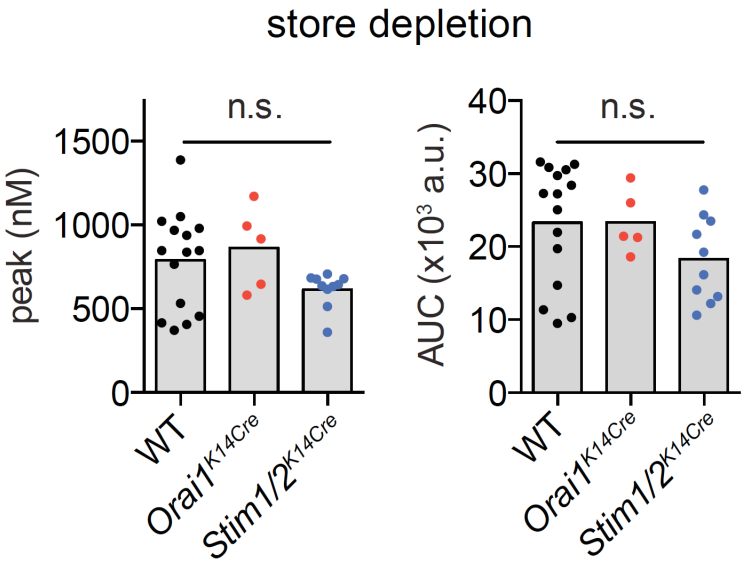

Supplemental Figure 3. Deletion of *Orai1* or *Stim1/Stim2* in murine sweat glands does not affect Ca^{2+} store depletion. Bar graphs quantify the peak $[Ca^{2+}]_i$ (left) and amount of Ca^{2+} released from ER stores (as the area under the curve, AUC, right) from experiments shown in Figure 3. The AUC was determined from 80-400 s. Each dot represents one gland of an individual mouse and bars represent mean values. No significant (n.s.) differences between genotypes were observed by one-way ANOVA statistical analysis using multiple comparisons. For additional details see Figure 3.

Supplemental Figure 4

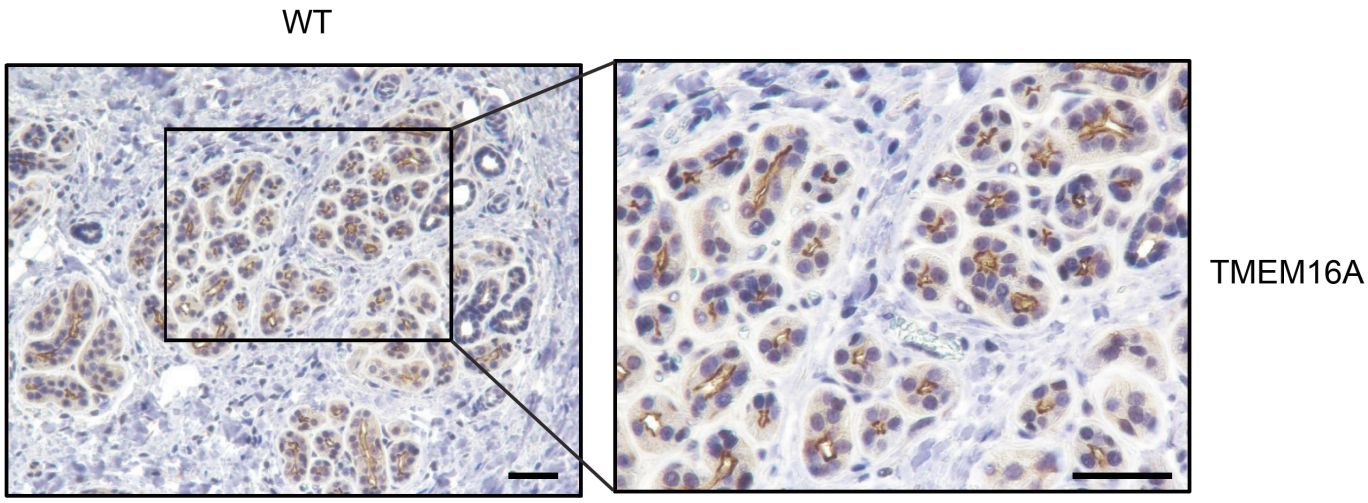

Supplemental Figure 4. TMEM16A is expressed in the apical membrane of secretory sweat gland cells in mice. Representative immunohistochemical staining of TMEM16A in footpad skin sections of WT mice. Images are representative of *n* = 2 WT mice. Scale bars, 50 μm.

Supplemental Figure 5

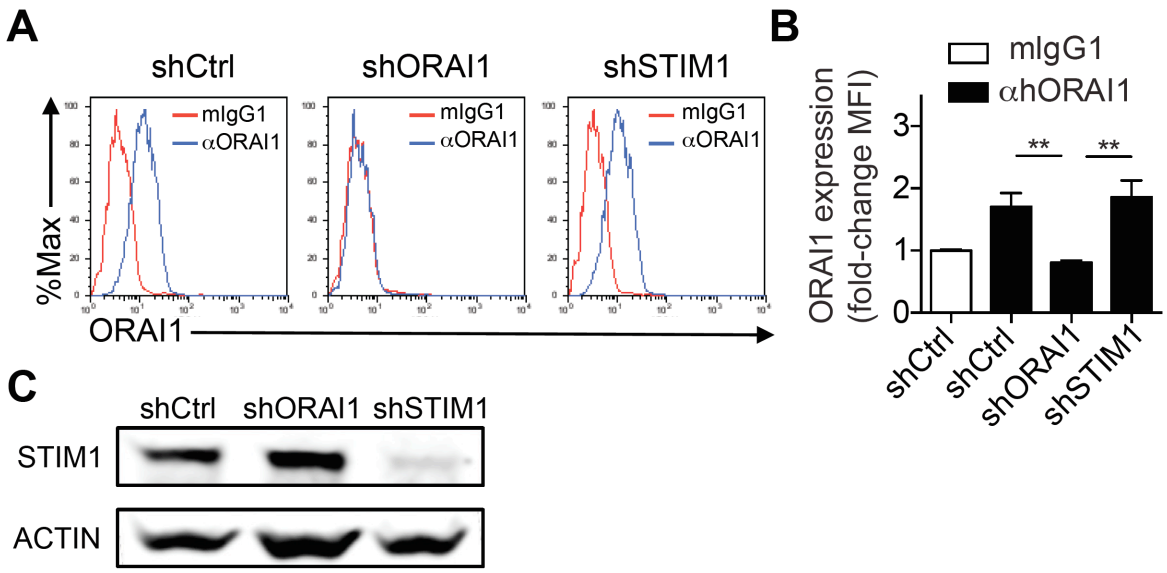

Supplemental Figure 5. shRNA-mediated knockdown of ORAI1 and STIM1 proteins in NCL-SG3 cells. (**A** and **B**) Representative flow cytometry histograms (**A**) and quantification (**B**) of ORAI1 expression on the surface of NCL-SG3 cells. ORAI1 expression was absent in NCL-SG3 cells stably transduced with shORAI1. ORAI1 was detected using a mouse anti-human monoclonal antibody that recognizes the second extracellular loop of ORAI1. Isotype: mouse IgG1 isotype control. Data in **B** are the mean ± SEM of 6 independent experiments. ***P*<0.01, by Student's 2-tailed *t* test. (**C**) Western blot showing the expression of STIM1 in protein lysates of NCL-SG3 cell lines. STIM1 detection was strongly reduced in NCL-SG3 cells stably transduced with shSTIM1. STIM1 was detected using a rabbit anti-human polyclonal antibody that recognizes the C terminus of STIM1. Goat-anti-actin polyclonal antibody was used as loading control; for the actin blot, replicate samples were run on a parallel gel. Images are representative of two independent experiments.

Supplemental Figure 6

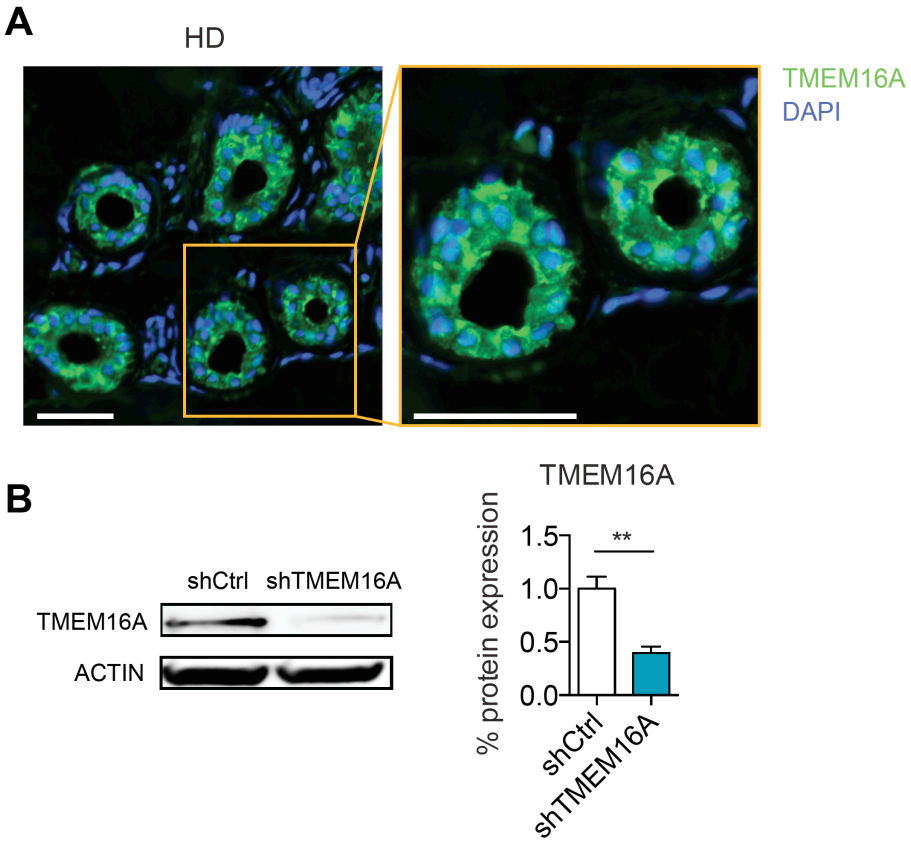

Supplemental Figure 6. TMEM16A is expressed in human eccrine sweat glands. (A) Protein expression and localization of TMEM16A in human eccrine sweat glands by immunofluorescence. Eccrine sweat glands from a healthy donor (HD) were stained with antibodies against human TMEM16A (green) and nuclei were counterstained with DAPI (blue). Images are representative of two independent experiments. The same pattern of TMEM16A distribution was observed using an antibody against mouse TMEM16A (for details see Methods). Scale bars, 50 µm. (**B**) Western blot analysis showing the expression (left) and quantification (right) of TMEM16A in protein lysates of NCL-SG3 cell lines transduced with shRNA control (shCtrl) or shTMEM16A. TMEM16A detection was strongly reduced in NCL-SG3 cells stably transduced with shTMEM16A. TMEM16A was detected using a rabbit anti-human polyclonal antibody as shown in **A**, which recognizes amino acids 828-877 of human TMEM16A. Goat-anti-actin polyclonal antibody was used as loading control. Data are representative of 5 independent experiments.

Supplemental Figure 7

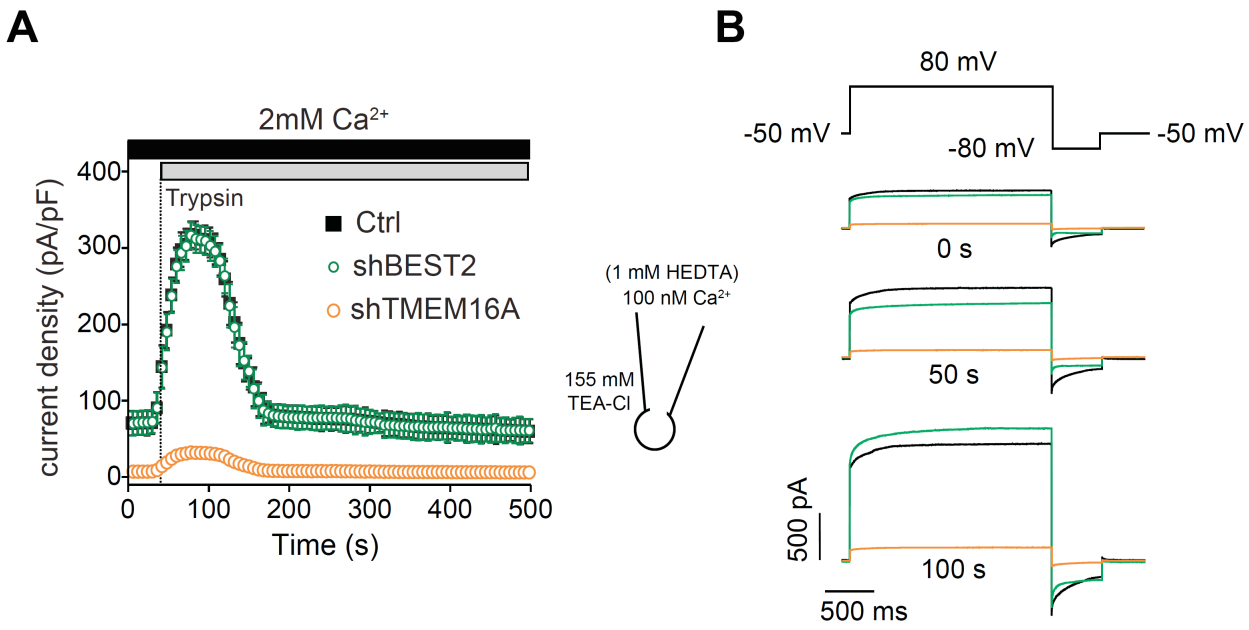

Supplemental Figure 7. CaCC currents in human sweat gland cells are mediated by TMEM16A. (**A**) Current densities in NCL-SG3 cells left untransduced (Ctrl), transduced with shTMEM16A or transduced with shBEST2. Cells were stimulated with 10 µM trypsin in extracellular buffer containing 2 mM Ca^{2+}. Internal pipette solution contained 1 mM HEDTA and 20 µM $CaCl_2$ to yield a physiological $[Ca^{2+}]_i$ of 100 nM. Currents were elicited by consecutive 2-s voltage steps to 80 mV, followed by a 0.5-s hyperpolarizing step to -80 mV. Data are the mean ± SEM of 5 untransduced control NCL-SG3 cells, 5 shBEST2 transduced cells and 5 shTMEM16A transduced cells. (**B**) Representative Cl^- current traces from individual Ctrl NCL-SG3 cells (black), shBEST2 (green) or shTMEM16A (orange), extracted at 0 s, 50 s and 100 s from the experiment shown in **A**.